Neurobiology of Aging 139 (2024) 73–81

Contents lists available at ScienceDirect

Neurobiology of Aging

journal homepage: www.elsevier.com/locate/neuaging.org

Brain age of rhesus macaques over the lifespan

Yang S. Liu [a,1], Madhura Baxi [b,1], Christopher R. Madan [c], Kevin Zhan [a], Nikolaos Makris [d], Douglas L. Rosene [e], Ronald J. Killiany [e,†], Suheyla Cetin-Karayumak [b,f], Ofer Pasternak [b,g], Marek Kubicki [b,d,f,2], Bo Cao [a,h,*,2]

[a] Department of Psychiatry, University of Alberta, Edmonton, AB, Canada
[b] Department of Psychiatry, Brigham and Women's Hospital, Harvard Medical School, Boston, MA, USA
[c] School of Psychology, University of Nottingham, Nottingham, UK
[d] Department of Psychiatry, Center for Morphometric Analysis, A. Martinos Center for Biomedical Imaging, Massachusetts General Hospital, Harvard Medical School, Boston, MA, USA
[e] Department of Anatomy & Neurobiology, Boston University Chobanian & Avedisian School of Medicine, Boston, MA, USA
[f] Laboratory of Mathematics in Imaging, Brigham and Women's Hospital, Harvard Medical School, Boston, MA, USA
[g] Department of Radiology, Brigham and Women's Hospital, Harvard Medical School, Boston, MA, USA
[h] Department of Computing Science, University of Alberta, Edmonton, AB, Canada

ARTICLE INFO

Keywords:
Aging
Machine learning
Rhesus macaque
Brain age

ABSTRACT

Through the application of machine learning algorithms to neuroimaging data the brain age methodology was shown to provide a useful individual-level biological age prediction and identify key brain regions responsible for the prediction. In this study, we present the methodology of constructing a rhesus macaque brain age model using a machine learning algorithm and discuss the key predictive brain regions in comparison to the human brain, to shed light on cross-species primate similarities and differences. Structural information of the brain (e.g., parcellated volumes) from brain magnetic resonance imaging of 43 rhesus macaques were used to develop brain atlas-based features to build a brain age model that predicts biological age. The best-performing model used 22 selected features and achieved an R^2 of 0.72. We also identified interpretable predictive brain features including Right Fronto-orbital Cortex, Right Frontal Pole, Right Inferior Lateral Parietal Cortex, and Bilateral Posterior Central Operculum. Our findings provide converging evidence of the parallel and comparable brain regions responsible for both non-human primates and human biological age prediction.

1. Introduction

The concept of biological age, as opposed to chronological age, has been extensively developed in the past two decades, where biomarkers of aging are derived based on complex interactions of factors such as environmental, epigenetic, physiological, neuroanatomical, and cognitive measures (Bae et al., 2013; Cao et al., 2015; Chen et al., 2015; Franke et al., 2017; Franke and Gaser, 2019; Hannum et al., 2013; Horvath, 2013; Madan and Kensinger, 2018; Park et al., 2002; Reagh and Yassa, 2017; Salthouse, 2011; Small et al., 2011; Walhovd et al., 2011). Brain age, a magnetic resonance imaging (MRI) based estimate of the biological age of the brain, has received increasing attention due to advancements in neuroimaging technology. Brain age can be based on structural and functional scans of the brain, obtained through non-invasive technologies such as MRI, functional MRI (fMRI), and diffusion tensor imaging (DTI) (for a review, see Franke and Gaser, 2019). Brain age is calculated by establishing a normative baseline for the general population, and using deviation from the normative baseline to identify subject-specific health characteristics and risk patterns for various age-related diseases such as Alzheimer's Disease (AD) and other psychiatric illnesses (Cole and Franke, 2017). This deviation from baseline might also be useful for monitoring and evaluating clinical assessments and the efficacy of interventions associated with aging.

It has already been well established that gray and white matter

* Correspondence to: Department of Psychiatry, University of Alberta, Edmonton, AB T6G 2B7, Canada.
E-mail address: cloudbocao@gmail.com (B. Cao).
[1] These authors contributed equally to this work as joint first authors
[2] These authors contributed equally to this work as joint senior authors
[†] The author is deceased.

https://doi.org/10.1016/j.neurobiolaging.2024.02.014
Received 11 September 2023; Received in revised form 27 February 2024; Accepted 28 February 2024
Available online 9 March 2024

volumes in the human brain generally decline with age (Cole and Franke, 2017) in areas of the cerebral cortex, and in some subcortical regions (Cao et al., 2015; Frangou et al., 2021; Madan and Kensinger, 2017). However, a challenge with brain age modeling is that age-related brain structural changes are not uniform across the brain, requiring multivariate approaches to model the trajectory of brain aging. Additional machine learning algorithms are then required to predict biological age at the individual subject level (Cao et al., 2015; Jiang et al., 2020; Madan, 2019; Madan and Kensinger, 2018; Schnack et al., 2016). These models are relatively robust thanks to applying cross-validation techniques that prevent overfitting and provide more accurate estimates of predictive validity (Bzdok et al., 2018).

Developing a comparative approach to studying aging with non-human primates (NHP) may provide insights into how generalizable patterns of structural changes are across species. Particularly, rhesus macaques are the most related species to humans besides the apes and by far the most commonly researched species for biomedical studies (Finch and Austad, 2012), the outcome of which may be generalizable to humans or be used to understand human-specific signatures. Also, rhesus macaques share similar aging profiles to humans, are less affected by clinical-grade cognitive declines such as AD, and are easier to study in laboratory environments due to their shorter lifespan than humans (Didier et al., 2016; Sridharan et al., 2012).

Similar to humans, age-related brain changes in NHP are also not uniform. Age-related decline in cortical volume and thickness has been found in chimpanzees (Autrey et al., 2014; Chen et al., 2013) and rhesus macaques (Chen et al., 2013; Koo et al., 2012; Kubicki et al., 2019; Moss et al., 1999). However, in chimpanzees, while some studies reported no decline in brain volume (Sherwood et al., 2011), other studies found a relationship between white matter volume and age that is best modeled with a cubic function (Autrey et al., 2014; Chen et al., 2013). In addition, many NHP subcortical structures peak during puberty and decline during aging (Sawiak et al., 2018). Nevertheless, subcortical regions such as the hippocampus and basal ganglia, which are strong predictors of aging in humans, are less robust predictors of aging in NHP, with inconsistent results across studies (Alexander et al., 2008; Shamy et al., 2011, 2006). The difference between humans and NHP could be attributed to differences between species in the organization of subcortical brain structures, their connections and their microstructure (Passingham, 2009).

Volumetric correlates of brain regions to age have been previously conducted on NHP including chimpanzees, rhesus macaques, and mouse lemurs (Autrey et al., 2014; Chen et al., 2013; Sawiak et al., 2014; Shamy et al., 2011; Sridharan et al., 2012). Given these findings, it is essential to establish whether the brain age methodologies applied on humans could be successfully duplicated to NHPs with reasonable predictive accuracy. Further, we can inquire whether changes in the brain regions are capable of predicting individual-level brain age and whether these changes align with findings from brain age literature in both humans and NHP. To date, the only NHP brain age model was conducted on baboons' MRI scans (Franke et al., 2017) where predictive brain aging models were built using MRI voxel-based morphometry. Franke et al. (2017) reported a general gray matter volume decline and white matter volume increase as baboons age; however, the study was not focused on identifying individual brain regions associated with brain age. Notably, voxel-based morphometry could be difficult to interpret across species, whereas an atlas-based parcellation method may be more interpretable, and further enable direct comparison of brain region features to similar regions in human brain age models (Madan and Kensinger, 2018), as well as to previous NHP studies of brain volumetric correlates of age.

In this study, we aim to build a brain age model with atlas-based brain volume parcellation using rhesus macaque MRI scans, to identify individual brain regions' contribution to age prediction and to compare them with findings from the human literature. We trained a machine learning model using brain region volumes derived from brain scans of 43 rhesus macaque monkeys to predict chronological age, and explored the regions that were driving the model's prediction. The motivation for our research is rooted in the goal of better understanding the aging process in the brain across species. We seek to explore whether the brain age concept applied to humans can be successfully replicated in NHPs and to identify the brain regions that contribute to individual-level brain age predictions. The findings from this study will enhance our understanding of brain aging with a greater emphasis on neurobiology through comparative analogues.

2. Methods

2.1. Rhesus macaque demographics

For this study, MRI scans were performed on 43 adult rhesus monkeys (25 females and 18 males). The ages of the monkeys ranged from 4 to 27 years with the average age being 17.58 for females and 11.61 for males. As rhesus macaques age at around a 1:3 ratio compared to humans, this is equivalent to humans 12–81 years of age (Tigges et al., 1988). The MRI scans used here are the same as those used in a previous study (Kubicki et al., 2019) which analyzed white matter development and correlations with aging.

2.2. Data acquisition & preprocessing

Detailed information on data acquisition and preprocessing procedures can be found in a previously published paper (Kubicki et al., 2019). Briefly, imaging data for anesthetized monkeys were acquired at two different sites.

Site 1. 21 monkeys (12 females and 9 males) were scanned, using a 3 T Siemens Allegra MRI at the Athinoula A. Martinos Center for Biomedical Imaging, Massachusetts General Hospital (MGH). Scan parameters were as follows: MP-RAGE structural MRI (sMRI) T1-weighted scan: Relaxation Time (TR) = 2530 ms, Echo Time (TE) = 3.36 ms, flip angle = 7 degrees, 128 coronal slices with 0.78 mm thickness (no gap), data matrix = 256 mm x 256 mm, Field of View (FOV) = 200 mm x 200 mm.

Site 2. 23 monkeys (14 females and 9 males) were scanned using a 3 T Philips Achieva MRI at the Boston University Medical Campus (BU). Scan parameters were as follows: MP-RAGE sMRI T1-weighted scan: TR = 7.09 ms, TE = 3.17 ms, flip angle = 8 degrees, 130 coronal slices with 0.6 mm thickness (no gap), data matrix = 256 mm x 256 mm, FOV = 153 mm x 153 mm.

T1-weighted scans for all monkeys underwent skull-stripping and motion correction using Functional Magnetic Resonance Imaging of the Brain (FMRIB) Software Library (FSL) software (http://www.fmrib.ox.ac. uk/fsl). These T1-weighted scans were then registered to the template space (pre-selected representative subject) using Advanced Normalization Tools (ANTs) registration (Avants et al., 2014; Kubicki et al., 2019). Next, the Center for Morphometric Analysis (CMA) cerebral cortex atlas of the macaque (Makris et al., 2010) and, the CMA digitized atlas of the macaque cerebral white matter fiber pathways (modified from Schmachmann and Pandya, "Fiber Pathways of the Brain", 2006, Oxford University Press) were registered to the T1-weighted scans for all monkeys. This allowed the computing of sMRI based imaging measures for different anatomical regions (ROIs).

2.3. Computing sMRI regional measures

Volumes of regions in the grey and white matter were computed using T1-weighted scans for the parcellated brain areas based on the registered CMA atlas, which was guided by the Schmahmann and Pandya's definitions and locations of cerebral fiber tracts (Makris et al., 2010; Petrides and Pandya, 2006) (Schmachmann and Pandya, "Fiber Pathways of the Brain", 2006, Oxford University Press). Regional volumes of grey and white matter areas were computed by multiplying the number of voxels in each of the ROI with the resolution of the voxel of

the T1-weighted scans. From the T1-weighted scans, the volumes (mm^3) for following brain areas were computed using the CMA atlas for each side of the brain hemisphere, including WM regions: Arcuate Fasciculus (AF), Cingulum Bundle (CB), Corpus Callosum (CC), Corticospinal Tract (ICpI), dorsal occipital bundle (DOB), External Capsule (EC), Extreme Capsule (EmC), fibers of the extreme capsule - Superior Longitudinal Fasciculus II (fEmC-SLF II), fibers of the extreme capsule (fEmC), fronto-occipital fasciculus (FOF), Inferior Longitudinal Fasciculus (ILF), Middle Longitudinal Fasciculus (MdLF), Muratoff Bundle (MB), Posterior Limb of Internal capsule (PB), Sagittal Stratum (SS), Striatal Bundle (StB), subcortical bundle (SB), Superior Longitudinal Fasciculus I (SLF I), Superior Longitudinal Fasciculus II - fibers of the accurate fasciculus (SLF II-fAF), Superior Longitudinal Fasciculus II (SLF II), Superior Longitudinal Fasciculus III (SLF III), Thalamic Bundle (TB), Uncinate Fasciculus (UF), Anterior Commissure (AC); and GM regions: Anterior Cingulate Gyrus Cortex (CGa), Basal Forebrain (BSF), Central Operculum (COa), Dorsolateral Striate Cortex (STRdl), Dorsolateral Superior Frontal Gyrus (F1dl), Dorsomedial Superior Frontal Gyrus (F1dm), Frontal Orbital Cortex (FOC), Frontal Pole (FP), Hypothalamus, Inferior Frontal Gyrus (F2), Inferior Lateral Parietal Cortex (LPCi), Inferior Temporal Gyrus (ITG), insula (INS), Medial Prefrontal Cortex (MPC), Medial Striate Cortex (STRM), Parahippocampal Gyrus (PH), Parietal Operculum (PO), Postcentral Gyrus (POG), Posterior Central Operculum (COp), Posterior Cingulate Gyrus (CGp), Precentral Gyrus (PRG), Prelunate Gyrus (PRL),Subcallosal Cortex (SC), Temporal Pole (TP), Ventral Medial Occipital Cortex (VMO), Superior Lateral Parietal Cortex (LPCs), Superior Temporal Gyrus (STG), Supratemporal Plane (STP). Volumes of bilateral brain regions were parcellated as separate ROIs (left- and right-). Brain regions not listed above were not available in the study dataset.

2.4. Rhesus macaque brain age index

Brain age is a composite index of brain volume changes during aging, built as a computational predictive model, and can be used to predict the chronological age of the subjects.

The concept of brain age index has been validated using human structural MRI data using both cross-sectional (Sivera et al., 2019) and longitudinal data (Cao et al., 2015), where atlas-based anatomical regions of the brain have been parcellated and adapted as predictive features of machine learning based models (e.g., regularized regression).

The rhesus macaque brain age index has been developed following the same concept. Predictive models are trained using brain volumetric data with the goal of predicting chronological age, with its generalizability tested on unseen data. The model-predicted chronological age is defined as the biological brain age.

2.5. Machine learning analysis

Machine learning analysis was conducted using python programming language 3.8.5, and the scikit-learn 1.0.1 python package and correlation analysis was conducted using the scipy package. The macaque brain age index was derived using a ridge regression model. Ridge regression is a popular parameter estimation method applied to regression to regularize the size of regression coefficients, and can effectively handle multicollinearity problems, reduce overfitting, and perform well when the feature dimension is larger than the sample size (Cessie & Houwelingen, 1992). Rhesus macaque's chronological age was used as the dependent variable. Fifty-six grey matter volumes and forty-eight white matter volumes of brain regions were converted to Z-scores (across each scanner separately) and used as input features to the brain age prediction model. Binary-coded scanner and sex variables were used as additional input features, where the scanner variable was included to remove any remaining site effects. Leave-one-out (LOO) cross-validation was used to assess model generalizability for both feature selection and the subsequent development of the brain age index, where 42 rhesus macaques were used as training data and one was held out for testing, iterating through all 43 subjects. Ridge regression coefficients of the 43 ridge regression models for LOO cross-validation were averaged to estimate the importance of each brain region in predicting age. A higher magnitude of the averaged coefficient indicates higher feature importance. We then further validate the feature importance against Pearson's correlation coefficient of the volume of each region to the age of the monkey.

2.6. Feature selection

Due to the relatively small sample size in our rhesus macaque dataset ($n = 43$) and a large number of features (108), reducing the number of features is essential to minimize overfitting. During the training of each LOO iteration, we used the Recursive Feature Elimination (RFE) with cross-validation (RFECV) (Guyon et al., 2002) algorithm to select the optimal number of features, by using the RFECV function from scikit-learn package. RFE is a feature selection method that iteratively removes the least relevant features to find the best number of features for making a prediction. Ridge regression was used as an estimator for each of the 5 internal RFE cross-validations and the number of features was optimized for the highest r^2. Then the selected features were used to fit a Ridge Regression model on the training data for this specific iteration. An internal 5-fold cross-validation was used for tuning the regularization strength hyperparameter α. This process was repeated 43 times until every monkey was left out as the testing data once. Among 43 models fitted, features consistently selected in all models were later used to build the rhesus macaque brain age index.

2.7. Brain age index

Following feature selection, the rhesus macaque brain age index was developed by fitting a Ridge Regression model using the selected features. The hyperparameter's value was selected by a 5-fold internal CV, optimizing for r^2. LOO cross-validation was performed using selected features to further confirm prediction generalizability.

2.8. Age span analysis

Using the full study sample, we performed a two-tailed t-test for the difference score of age-index-predicted and the chronological age to test the hypothesis if the mean is equal to zero. A significant t-test would suggest potential model prediction bias across age span. We then grouped the monkeys into a young group and an old group and conducted the same t-tests for the difference scores within each group. A significant t-test would suggest the differential presence of regression attenuation modulated by maturation.

3. Results

The models built from training data in the feature selection procedure consistently predict rhesus macaque's age ($R^2 = 0.65$, Mean Absolute Error (MAE) = 3.31). The refitted brain age index model using selected features consistently predicts the rhesus macaque's age ($R^2 = 0.72$, MAE = 2.91) (Figure 1). Twenty-two features were selected across all 43 iterations of LOO cross-validation (Figure 2). Fig. 2 B shows a 3D visualization of the GM regions (Madan, 2015; Pernet & Madan, 2020)

The goal of building a predictive model is to optimize its predictive performance instead of model interpretation. To facilitate accurate model interpretation, we took a conservative approach to only focus on interpreting variables significantly correlated with age, and with congruent correlation coefficient and feature importance (i.e., both the correlation and feature importance signs are positive, or both are negative). Out of 22 model selected features, seven features were identified to have a significant negative correlation with Age and were congruent with feature importance. Other model selected brain regions

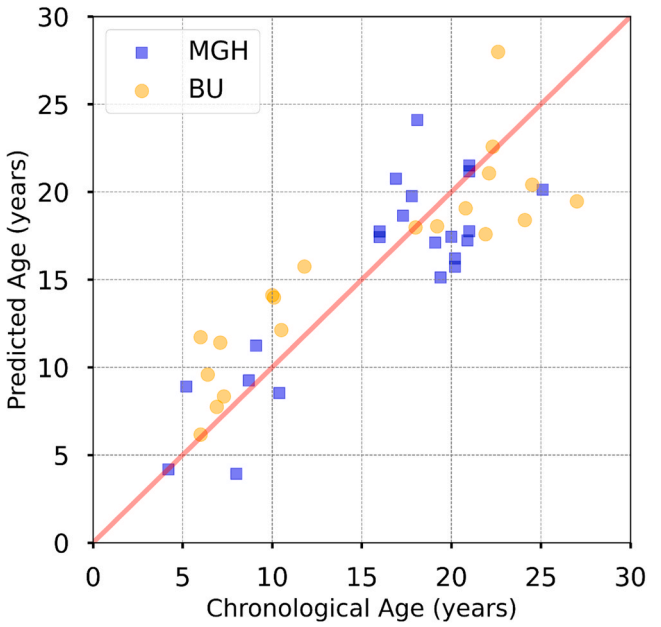

Fig. 1. Chronological age as a function of model-predicted age. MGH: Massachusetts General Hospital, BU: Boston University Medical Center. The plot is based on LOOCV results. The middle line on the plot is a reference line to indicate when chronological age and predicted age are equal. The model overpredicts age when the data point is above the line, and underpredicts age when the data point is below the line.

did not meet the selection criteria. For grey matter regions, the FOC, superior and inferior parts of the lateral parietal cortex, Bilateral central operculum, frontal pole (FP), and subcallosal cortex were identified as significant predictive biomarkers for aging in rhesus macaques. For white matter regions, only the fibers of the extreme capsule and the uncinate fasciculus were significant predictive biomarkers for aging. In addition, sex can facilitate the prediction of age, where being male predicts younger age (Table 1). However, this could be a consequence of the consistency of the set of monkeys utilized in the data.

For the age span analysis, we found no evidence of overall prediction bias. The predicted age and chronological age difference score is not different from zero ($t = -0.45$, $df = 42$, $p = .0653$). The difference scores were not different from zero in the young ($t = 1.49$, $df = 16$, $p = .155$) and old group ($t = -1.83$, $df = 25$, $p = .080$). Out of 43 rhesus macaques, 53.5% (23 out of 43) of the monkeys were predicted to be older than their chronological age, consistent with the statistical conclusion of no overall attenuation of the slope.

4. Discussion

In this study, we successfully developed a rhesus macaque brain age index using parcellated WM and GM volumes to predict chronological age in rhesus macaques ($R^2 = 0.72$), while controlling for sex and study sites. Also, we identified a list of GM and WM regions that were consistent predictors (with cross validation) of biological age. The identified brain regions were generally aligned with the literature showing association of volumetric change of brain regions with age in both humans (Bagarinao et al., 2018; Good et al., 2001; Grieve et al., 2005; Sala et al., 2012; Taki et al., 2011) and NHP (Alexander et al., 2008; Autrey et al., 2014; Chen et al., 2013; Wisco et al., 2008), including in postmortem studies (Herndon et al., 1999). Our results support the generalizability of the brain age concept between humans and NHP, using atlas-based MRI features and machine learning.

4.1. Comparison with human age models

Predicting chronological age from neuroimaging data has been an increasingly popular topic in human studies. A large positive difference between predicted age and chronological age might suggest implications of brain disorders such as schizophrenia or Alzheimer's disease. Although brain age models have been developed and validated using large human datasets, this approach has not yet been widely studied using non-human primate (NHP) data. As rhesus macaques are used as translational models for aging and neurodegeneration (Bagarinao et al., 2018; Hara et al., 2012; Herndon et al., 1997; Mattison et al., 2017; Moore et al., 2006; Stonebarger et al., 2020; Uno, 1993), investigating brain aging across primate species is increasingly valuable.

To our knowledge, we are the first to develop a brain age machine learning model for rhesus macaques. Compared to brain age models in baboons ($R^2 = 0.62$), our model's performance ($R^2 = 0.72$) is proficient and has the advantage of allowing interpretability of brain region features (Franke et al., 2017).

Human studies examining cortical and subcortical structures involved in brain aging typically have larger sample sizes and are able to leverage deep learning to achieve high accuracy. Levakov et al. have used a CNN model on 10,176 human MRI images of a large composite dataset for brain age prediction with high accuracy ($R^2 = 0.96$, Levakov et al., 2020). However, there is a "black box" problem that it is often difficult to analyze and interpret their findings due to the complex structure of machine learning models as they are composed of hundreds of thousands of abstract parameters. In addition, very high accuracy in predictive models may limit the practical application of brain age index as there's a diminishing unexplained variance from the model.

An advantage of our study lies in how we have determined and discussed prominent brain regions that contributed most to the final prediction. The areas determined to be significant by our model are consistent with findings on human aging where frontal white matter volumes noticeably decline with age (Gunning-Dixon et al., 2009). Additionally, human frontal cortical, as well as subcortical structures, decline linearly with aging in humans (Bozzali et al., 2008). This supports our model with a higher predictive ability of brain regions such as the FOC and FP.

Nonetheless, the generalizability of the model to humans or other NHPs should be investigated further as differences in both brain maturation and aging timelines and organization might hinder the ability of accurate prediction.

4.1.1. Model selected white matter regions

White matter tracts in humans increase in volume until the age of 20 (Knickmeyer et al., 2008), and deteriorate most quickly and evidently starting at around 50 years of age (Raz et al., 2005; Salat et al., 1999). In macaques and NHP, WM volume has a stronger correlation with age than GM volume (Wisco et al., 2008). With human WM, there are regional areas with relatively accelerated decrease or preservation in volume (Good et al., 2001). However, regional volumetric changes in macaque WM have not been explored in-depth in terms of their correlation to aging. This is partially because studies using diffusion tensor imaging (DTI) are able to detect WM microstructure degeneration with aging at an earlier age. A decline in WM microstructure typically precedes WM volume loss in humans (Westlye et al., 2010). With the penalized regression model, we show that relative losses or preservation in WM volume in certain areas are predictive of aging.

The right Uncinate Fasciculus (UF) is a white matter tract that connects the frontal lobe with the anterior temporal lobe. While not much literature identifies a decline of volume in the UF in macaques (Makris et al., 2007; Sandell and Peters, 2003; Shobin et al., 2017), in human studies, the volume of the UF was seen to be linearly increasing in developing healthy children as well as negatively correlated at old ages (Hasan et al., 2009), and was found to have a significant correlation with age in a cubic relationship (Eluvathingal et al., 2007; Hasan et al., 2009;

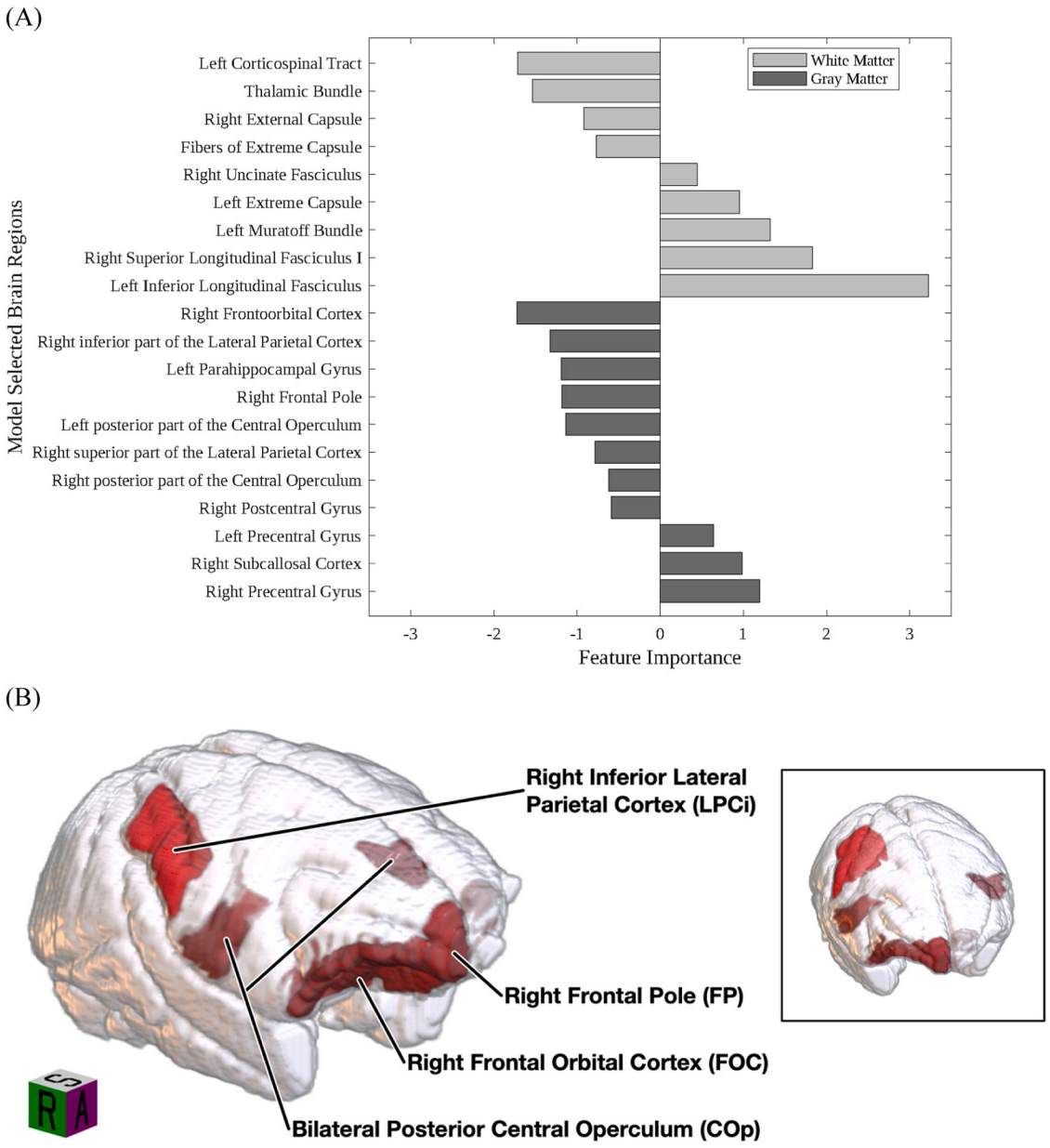

Fig. 2. Summary of model-selected brain regions as age predictors. (A) Feature importance values for predictors, selected by brain age index, for white matter and gray matter regions separately. (B) 3D visualization of gray matter regions with interpretable feature importance values. The cube in the bottom left shows the relative orientation of the main 3D render (R: right; A: anterior; S: superior). A second perspective from a more anterior view is shown inset.

Table 1
Interpretable predictive features ranked by models' averaged coefficient.

Feature	Correlation with Age	Feature Importance	p_{corr}
Right Fronto-orbital Cortex (FOC)	-0.65	-1.72	< 0.000
Right Inferior part of the Lateral Parietal Cortex	-0.46	-1.32	0.002
Sex (Male)	-0.40	-1.30	0.008
Right Frontal Pole	-0.45	-1.18	0.002
Left Posterior part of the Central Operculum	-0.35	-1.13	0.022
Right Fibers of Extreme Capsule	-0.34	-0.77	0.028
Right Posterior part of the Central Operculum	-0.48	-0.62	0.001

Feature importance is measured by the averaged ridge regression coefficients across all LOO folds. p_{corr} represents the p value of correlation coefficients.

Lebel et al., 2008). Our results indicated that the Extreme capsule is a predictor in our model for aging. Similar to the UF, volumetric studies of NHP brain aging have not identified it as predictive of normal aging (Makris et al., 2007; Sandell and Peters, 2003; Shobin et al., 2017). In the work of Taki et al. (2004), they found that the volume of the Extreme Capsule decreased during aging in humans. The left inferior (ILF) and right superior (SLF) longitudinal fasciculus are WM regions with high positive coefficients in the model. In humans, the microstructure integrity of the ILF and SLF share a "U-shaped" relationship with age as it increases early on and declines at older ages (Lebel and Beaulieu, 2011; Madhavan et al., 2014). However, the volume of the ILR and SLF remains relatively constant at older ages and shows a positive correlation at younger ages. An interesting finding of this study is that the volume of the projection fiber of the ICpl is a non-zero coefficient in the model. Studies have shown that the FA of this region remains constant with aging (Makris et al., 2007) and is a poor predictor for aging (Sala et al., 2012). However, with interactions between other brain regions of

WM and GM, we found the volume of the ICpl has a negative relationship with aging.

4.1.2. Model selected gray matter regions

Our findings support the prior evidence that grey matter regions that were found to be linked to aging in humans also decline in volume in aging rhesus macaques. Additionally, the model identifies grey matter regions in rhesus macaques that are strongly predictive of aging but have not been previously reported. The volume of the right fronto-orbital cortex (FOC) had the largest negative coefficient within the ridge regression model. The FOC is a key cortical area involved in decision-making and rational thought. In NHP, the volume of the FOC correlated negatively with aging (Alexander et al., 2008; Autrey et al., 2014; Uematsu et al., 2017) while in humans, the FOC was reported as a biomarker for older age and reduced executive function (Raz et al., 2010, 2005; Salat et al., 2001). Areas in the frontal lobe such as the FOC tend to have the most evident loss in volume due to aging and our model demonstrates that such volumetric changes can be predictive of aging in rhesus macaques.

Our findings also indicate that the right superior (LPCs) and right inferior parts (LPCi) of the lateral parietal cortex are predictive of aging. Although this has not been reported in rhesus macaque studies, it is consistent with the findings of human studies (Fjell et al., 2009; Salat et al., 2004). Similarly, a decrease in volume in the bilateral posterior central operculum (COp) has been previously described as correlated with human aging (Bagarinao et al., 2018; Good et al., 2001; Grieve et al., 2005; Taki et al., 2011) but has not been reported in the NHP literature. Since volumetric changes in NHP, compared to human brains, with aging are less robust, changes in the LPCs, LPCi and COp have a higher predictive value for NHP aging when analyzed together with other brain regions in the model. The bilateral precentral (PCG) and right postcentral gyrus (POG), among other identified predictive factors of aging, have been reported before with a significant negative correlation with aging in rhesus macaques (Koo et al., 2012) as well as human studies (Good et al., 2001; Grieve et al., 2005; Salat et al., 2004; Sowell et al., 2007; Taki et al., 2004).

In addition, our study also reports that the right frontal pole (FP) is a good predictor for aging. While not much evidence exists for a volumetric decrease in FP, studies have found a decrease in serotonin and acetylcholine levels in the FP of aged macaques (Wenk et al., 1989). Relative to the entire prefrontal cortex, the frontal pole was identified previously in human studies as lacking a significant correlation with aging (Douaud et al., 2014; Tisserand et al., 2002). We remark that although some brain regions such as the cingulate gyrus (Grieve et al., 2005) display a poor correlation with age and are relatively well preserved through normal aging, including them in the regression model improves its performance as it is able to account for some of the residuals of the model.

4.2. Model performance across life span

A key interest of the brain age prediction approach is to identify whether the brain age index performs uniformly across the life span. Brain age index using regression models may suffer from regression attenuation, where the slope of the model could be flattened due to measurement error (Cao et al., 2015). The wide range of age captured in our rhesus macaque sample opened an opportunity to evaluate across lifespan model performance. However, our analysis found no evidence of prediction bias over the life span. Though age-related changes in brain structure are known to be non-uniform, our results indicate no systematic bias in relation to lifespan, as shown in Figure 1.

Due to the relatively small sample size, the current results should be interpreted with caution and need further confirmation from future studies with a larger sample and formal statistical analysis.

4.3. Limitations

The current study is motivated to provide a proof of concept for an NHP brain age model trained using atlas-based features and to provide a cross-species comparison to the human brain age model using a similar methodology. One limitation of the current methodology is that we were not directly modeling the potential non-linear relationship between white and grey matter volume and brain age. This issue has been considered in both studies of humans (Fjell et al., 2009; Madan and Kensinger, 2018) and NHP studies. As such, the brain age index we built may miss some relevant features with non-linear relationships to age. However, evidence for non-linear relationships between age and volume for each individual brain region is still inconclusive. While there is support for the relationship between global GM and healthy human aging, this relationship was only significant as a linear model (Good et al., 2001). Individual cortical regions have been reported to have heterogeneous relationships with aging.

Additionally, due to the size and cross-sectional nature of the study, the younger and older age ranges could have been underrepresented compared to the middle age range for our subjects. This is something that a future study could examine with a larger sample size.

5. Conclusion

We report one of the first NHP brain age models using atlas-based MRI features and machine learning, which successfully identified prominent age prediction features, and validated the generalizability of the brain age concept. This line of findings spurs future interest in comparative studies of aging and provides converging evidence of the parallel and comparable brain regions responsible for both NHP and human biological age prediction.

CRediT authorship contribution statement

Yang S. Liu: Conceptualization, Methodology, Data curation, Funding acquisition, Investigation, Methodology, Visualization, Writing – original draft. **Madhura Baxi:** Data curation, Investigation, Methodology, Resources, Writing – original draft. **Christopher R. Madan:** Investigation, Methodology, Visualization, Writing – original draft, Writing – review & editing. **Kevin Zhan:** Investigation, Writing – review & editing. **Nikos Makris:** Resources, Writing – review & editing. **Douglas Rosene:** Resources, Writing – review & editing. **Ron Killiany:** Resources, Writing – review & editing. **Suheyla Cetin-Karayumak:** Resources, Writing - review & editing. **Ofer Pasternak:** Resources, Writing – review & editing. **Marek Kubicki:** Resources, Supervision, Writing – review & editing. **Bo Cao:** Conceptualization, Methodology, Funding acquisition, Supervision, Writing – review & editing.

Declaration of Competing Interest

The authors declare there is no conflict of interest.

Data availability

The data used in this research can be accessed by contacting the corresponding author upon reasonable request.

Acknowledgments

Dr. Ronald J Killiany, Department of Anatomy and Neurobiology, Boston University School of Medicine, passed away during the preparation of this manuscript. We acknowledge his generous help on this research project as a co-author. Behavioral studies and processing were conducted with the support of equipment from the Behavioural Analysis Platform SCAC (University of Rouen Normandy, France). Bo Cao is supported in part by the Canada Research Chairs program, NARSAD

Young Investigator Grant of The Brain & Behavior Research Foundation, Alberta Innovates, Mental Health Foundation, MITACS Accelerate program, Simon & Martina Sochatsky Fund for Mental Health, Howard Berger Memorial Schizophrenia Research Fund, the Abraham & Freda Berger Memorial Endowment Fund, the Alberta Synergies in Alzheimer's and Related Disorders (SynAD) program, University Hospital Foundation and University of Alberta. Yang S. Liu is supported in part by the Alberta Synergies in Alzheimer's and Related Disorders (SynAD) program which is funded by the Alzheimer Society of Alberta and Northwest Territories through their Hope for Tomorrow program, SynAD operates in partnership with the Neuroscience and Mental Health Institute at the University of Alberta. Yang S. Liu is also supported by the University Hospital Foundation and MITACS Accelerate program. Marek Kubicki, Madhura Baxi, Nikolaos Makris and Douglas L. Rosene are supported by National Institutes of Health Grants 5R01AG042512 and Grant RF1AG043640.

Submission declaration and verification

The authors of "Brain Age of Rhesus Macaques over the Lifespan" *declare that the work described has not been published previously and is not under consideration for publication elsewhere.* The work's publication is approved by all authors and tacitly or explicitly by the responsible authorities where the work was carried out, and that, if accepted, it will not be published elsewhere in the same form, in English or in any other language, including electronically without the written consent of the copyright-holder.

References

Alexander, G.E., Chen, K., Aschenbrenner, M., Merkley, T.L., Santerre-Lemmon, L.E., Shamy, J.L., Skaggs, W.E., Buonocore, M.H., Rapp, P.R., Barnes, C.A., 2008. Age-related regional network of magnetic resonance imaging gray matter in the rhesus macaque. J. Neurosci. 28, 2710–2718. https://doi.org/10.1523/JNEUROSCI.1852-07.2008.

Autrey, M.M., Reamer, L.A., Mareno, M.C., Sherwood, C.C., Herndon, J.G., Preuss, T., Schapiro, S.J., Hopkins, W.D., 2014. Age-related effects in the neocortical organization of chimpanzees: Gray and white matter volume, cortical thickness, and gyrification. NeuroImage 101, 59–67. https://doi.org/10.1016/j.neuroimage.2014.06.053.

Avants, B.B., Tustison, N.J., Stauffer, M., Song, G., Wu, B., Gee, J.C., 2014. The Insight ToolKit image registration framework. Front. Neuroinform. 8 https://doi.org/10.3389/fninf.2014.00044.

Bae, C.-Y., Kang, Y.G., Suh, Y.-S., Han, J.H., Kim, S.-S., Shim, K.W., 2013. A model for estimating body shape biological age based on clinical parameters associated with body composition. Clin. Interv. Aging 8 11–18. https://doi.org/10.2147/CIA.S38220.

Bagarinao, E., Watanabe, H., Maesawa, S., Mori, D., Hara, K., Kawabata, K., Yoneyama, N., Ohdake, R., Imai, K., Masuda, M., Yokoi, T., Ogura, A., Wakabayashi, T., Kuzuya, M., Ozaki, N., Hoshiyama, M., Isoda, H., Naganawa, S., Sobue, G., 2018. An unbiased data-driven age-related structural brain parcellation for the identification of intrinsic brain volume changes over the adult lifespan. NeuroImage 169, 134–144. https://doi.org/10.1016/j.neuroimage.2017.12.014.

Bozzali, M., Cercignani, M., Caltagirone, C., 2008. Brain volumetrics to investigate aging and the principal forms of degenerative cognitive decline: a brief review. Magn. Reson. Imaging, Proc. Int. Sch. Magn. Reson. Brain Funct. 26, 1065–1070. https://doi.org/10.1016/j.mri.2008.01.044.

Bzdok, D., Altman, N., Krzywinski, M., 2018. Statistics versus machine learning. Nat. Methods 15, 233–234. https://doi.org/10.1038/nmeth.4642.

Cao, B., Mwangi, B., Hasan, K.M., Selvaraj, S., Zeni, C.P., Zunta-Soares, G.B., Soares, J.C., 2015. Development and validation of a brain maturation index using longitudinal neuroanatomical scans. NeuroImage 117, 311–318. https://doi.org/10.1016/j.neuroimage.2015.05.071.

Cessie, S.L., Houwelingen, J.V., 1992. Ridge estimators in logistic regression. J. R. Stat. Soc. Ser. C: Appl. Stat. *41* (1), 191–201.

Chen, Weiyang, Qian, W., Wu, G., Chen, Weizhong, Xian, B., Chen, X., Cao, Y., Green, C. D., Zhao, F., Tang, K., Han, J.-D.J., 2015. Three-dimensional human facial morphologies as robust aging markers. Cell Res 25, 574–587. https://doi.org/10.1038/cr.2015.36.

Chen, X., Errangi, B., Li, L., Glasser, M.F., Westlye, L.T., Fjell, A.M., Walhovd, K.B., Hu, X., Herndon, J.G., Preuss, T.M., Rilling, J.K., 2013. Brain aging in humans, chimpanzees (Pan troglodytes), and rhesus macaques (Macaca mulatta): magnetic resonance imaging studies of macro- and microstructural changes. Neurobiol. Aging 34, 2248–2260. https://doi.org/10.1016/j.neurobiolaging.2013.03.028.

Cole, J.H., Franke, K., 2017. Predicting age using neuroimaging: innovative brain ageing biomarkers. Trends Neurosci. 40, 681–690. https://doi.org/10.1016/j.tins.2017.10.001.

Didier, E.S., MacLean, A.G., Mohan, M., Didier, P.J., Lackner, A.A., Kuroda, M.J., 2016. Contributions of Nonhuman Primates to Research on Aging. Vet. Pathol. 53, 277–290. https://doi.org/10.1177/0300985815622974.

Douaud, G., Groves, A.R., Tamnes, C.K., Westlye, L.T., Duff, E.P., Engvig, A., Walhovd, K. B., James, A., Gass, A., Monsch, A.U., Matthews, P.M., Fjell, A.M., Smith, S.M., Johansen-Berg, H., 2014. A common brain network links development, aging, and vulnerability to disease. Proc. Natl. Acad. Sci. 111, 17648–17653. https://doi.org/10.1073/pnas.1410378111.

Eluvathingal, T.J., Hasan, K.M., Kramer, L., Fletcher, J.M., Ewing-Cobbs, L., 2007. Quantitative diffusion tensor tractography of association and projection fibers in normally developing children and adolescents. Cereb. Cortex 17, 2760–2768. https://doi.org/10.1093/cercor/bhm003.

Finch, C.E., Austad, S.N., 2012. Primate aging in the mammalian scheme: the puzzle of extreme variation in brain aging. AGE 34, 1075–1091. https://doi.org/10.1007/s11357-011-9355-9.

Fjell, A.M., Walhovd, K.B., Fennema-Notestine, C., McEvoy, L.K., Hagler, D.J., Holland, D., Brewer, J.B., Dale, A.M., 2009. One-year brain atrophy evident in healthy aging. J. Neurosci. 29, 15223–15231. https://doi.org/10.1523/JNEUROSCI.3252-09.2009.

Frangou, S., Modabbernia, A., Williams, S.C.R., Papachristou, E., Doucet, G.E., Agartz, I., Aghajani, M., Akudjedu, T.N., Albajes-Eizagirre, A., Alnaes, D., Alpert, K.I., Andersson, M., Andreasen, N.C., Andreassen, O.A., Asherson, P., Banaschewski, T., Bargallo, N., Baumeister, S., Baur-Streubel, R., Bertolino, A., Bonvino, A., Boomsma, D.I., Borgwardt, S., Bourque, J., Brandeis, D., Breier, A., Brodaty, H., Brouwer, R.M., Buitelaar, J.K., Busatto, G.F., Buckner, R.L., Calhoun, V., Canales-Rodríguez, E.J., Cannon, D.M., Caseras, X., Castellanos, F.X., Cervenka, S., Chaim-Avancini, T.M., Ching, C.R.K., Chubar, V., Clark, V.P., Conrod, P., Conzelmann, A., Crespo-Facorro, B., Crivello, F., Crone, E.A., Dale, A.M., Dannlowski, U., Davey, C., de Geus, E.J.C., de Haan, L., de Zubicaray, G.I., den Braber, A., Dickie, E.W., Di Giorgio, A., Doan, N.T., Dørum, E.S., Ehrlich, S., Erk, S., Espeseth, T., Fatouros-Bergman, H., Fisher, S.E., Fouche, J.-P., Franke, B., Frodl, T., Fuentes-Claramonte, P., Glahn, D.C., Gotlib, I.H., Grabe, H.-J., Grimm, O., Groenewold, N.A., Grotegerd, D., Gruber, O., Gruner, P., Gur, R.E., Gur, R.C., Hahn, T., Harrison, B.J., Hartman, C.A., Hatton, S.N., Heinz, A., Heslenfeld, D.J., Hibar, D.P., Hickie, I.B., Ho, B.-C., Hoekstra, P.J., Hohmann, S., Holmes, A.J., Hoogman, M., Hosten, N., Howells, F.M., Hulshoff Pol, H.E., Huyser, C., Jahanshad, N., James, A., Jernigan, T. L., Jiang, J., Jönsson, E.G., Joska, J.A., Kahn, R., Kalnin, A., Kanai, R., Klein, M., Klyushnik, T.P., Koenders, L., Koops, S., Krämer, B., Kuntsi, J., Lagopoulos, J., Lázaro, L., Lebedeva, I., Lee, W.H., Lesch, K.-P., Lochner, C., Machielsen, M.W.J., Maingault, S., Martin, N.G., Martínez-Zalacaín, I., Mataix-Cols, D., Mazoyer, B., McDonald, C., McDonald, B.C., McIntosh, A.M., McMahon, K.L., McPhilemy, G., Meinert, S., Menchón, J.M., Medland, S.E., Meyer-Lindenberg, A., Naaijen, J., Najt, P., Nakao, T., Nordvik, J.E., Nyberg, L., Oosterlaan, J., de la Foz, V.O.-G., Paloyelis, Y., Pauli, P., Pergola, G., Pomarol-Clotet, E., Portella, M.J., Potkin, S.G., Radua, J., Reif, A., Rinker, D.A., Roffman, J.L., Rosa, P.G.P., Sacchet, M.D., Sachdev, P.S., Salvador, R., Sánchez-Juan, P., Sarró, S., Satterthwaite, T.D., Saykin, A.J., Serpa, M.H., Schmaal, L., Schnell, K., Schumann, G., Sim, K., Smoller, J. W., Sommer, I., Soriano-Mas, C., Stein, D.J., Strike, L.T., Swagerman, S.C., Tamnes, C.K., Temmingh, H.S., Thomopoulos, S.I., Tomyshev, A.S., Tordesillas-Gutiérrez, D., Trollor, J.N., Turner, J.A., Uhlmann, A., van den Heuvel, O.A., van den Meer, D., van der Wee, N.J.A., van Haren, N.E.M., van 't Ent, D., van Erp, T.G.M., Veer, I.M., Veltman, D.J., Voineskos, A., Völzke, H., Walter, H., Walton, E., Wang, L., Wang, Y., Wassink, T.H., Weber, B., Wen, W., West, J.D., Westlye, L.T., Whalley, H., Wierenga, L.M., Wittfeld, K., Wolf, D.H., Worker, A., Wright, M.J., Yang, K., Yoncheva, Y., Zanetti, M.V., Ziegler, G.C., , Karolinska Schizophrenia Project (KaSP), Thompson, P.M., Dima, D., 2021. Cortical thickness across the lifespan: Data from 17,075 healthy individuals aged 3-90 years. Hum. Brain Mapp. https://doi.org/10.1002/hbm.25364.

Franke, K., Bublak, P., Hoyer, D., Billiet, T., Gaser, C., Witte, O.W., Schwab, M., 2017. In vivo biomarkers of structural and functional brain development and aging in humans 27.

Franke, Katja, Clarke, G.D., Dahnke, R., Gaser, C., Kuo, A.H., Li, C., Schwab, M., Nathanielsz, P.W., 2017. Premature brain aging in baboons resulting from moderate fetal undernutrition. Front. Aging Neurosci. 9, 92. https://doi.org/10.3389/fnagi.2017.00092.

Franke, K., Gaser, C., 2019. Ten Years of BrainAGE as a neuroimaging biomarker of brain aging: what insights have we gained? Front. Neurol. 10 https://doi.org/10.3389/fneur.2019.00789.

Good, C.D., Johnsrude, I.S., Ashburner, J., Henson, R.N.A., Friston, K.J., Frackowiak, R.S. J., 2001. A voxel-based morphometric study of ageing in 465 normal adult human brains. NeuroImage 21–36.

Grieve, S.M., Clark, C.R., Williams, L.M., Peduto, A.J., Gordon, E., 2005. Preservation of limbic and paralimbic structures in aging. Hum. Brain Mapp. 25, 391–401. https://doi.org/10.1002/hbm.20115.

Gunning-Dixon, F.M., Brickman, A.M., Cheng, J.C., Alexopoulos, G.S., 2009. Aging of cerebral white matter: a review of MRI findings. Int. J. Geriatr. Psychiatry 24, 109–117. https://doi.org/10.1002/gps.2087.

Guyon, I., Weston, J., Barnhill, S., Vapnik, V., 2002. Gene selection for cancer classification using support vector machines. Mach. Learn. 46, 389–422. https://doi.org/10.1023/A:1012487302797.

Hannum, G., Guinney, J., Zhao, L., Zhang, L., Hughes, G., Sadda, S., Klotzle, B., Bibikova, M., Fan, J.-B., Gao, Y., Deconde, R., Chen, M., Rajapakse, I., Friend, S., Ideker, T., Zhang, K., 2013. Genome-wide methylation profiles reveal quantitative views of human aging rates. Mol. Cell 49, 359–367. https://doi.org/10.1016/j.molcel.2012.10.016.

Hara, Y., Rapp, P.R., Morrison, J.H., 2012. Neuronal and morphological bases of cognitive decline in aged rhesus monkeys. AGE 34, 1051–1073. https://doi.org/10.1007/s11357-011-9278-5.
Hasan, K.M., Iftikhar, A., Kamali, A., Kramer, L.A., Ashtari, M., Cirino, P.T., Papanicolaou, A.C., Fletcher, J.M., Ewing-Cobbs, L., 2009. Development and aging of the healthy human brain uncinate fasciculus across the lifespan using diffusion tensor tractography. Brain Res 1276, 67–76. https://doi.org/10.1016/j.brainres.2009.04.025.
Herndon, J.G., Moss, M.B., Rosene, D.L., Killiany, R.J., 1997. Patterns of cognitive decline in aged rhesus monkeys. Behav. Brain Res. 87, 25–34. https://doi.org/10.1016/S0166-4328(96)02256-5.
Herndon, J.G., Tigges, J., Anderson, D.C., Klumpp, S.A., McClure, H.M., 1999. Brain weight throughout the life span of the chimpanzee. J. Comp. Neurol. 409, 567–572 https://doi.org/10.1002/(SICI)1096-9861(19990712)409:4<567::AID-CNE4>3.0.CO;2-J.
Horvath, S., 2013. DNA methylation age of human tissues and cell types. Genome Biol. 14, 3156.
Jiang, H., Lu, N., Chen, K., Yao, L., Li, K., Zhang, J., Guo, X., 2020. Predicting brain age of healthy adults based on structural MRI parcellation using convolutional neural networks. Front. Neurol. 0 https://doi.org/10.3389/fneur.2019.01346.
Knickmeyer, R.C., Gouttard, S., Kang, C., Evans, D., Wilber, K., Smith, J.K., Hamer, R.M., Lin, W., Gerig, G., Gilmore, J.H., 2008. A structural MRI study of human brain development from birth to 2 years. J. Neurosci. 28, 12176–12182. https://doi.org/10.1523/JNEUROSCI.3479-08.2008.
Koo, B.-B., Schettler, S.P., Murray, D.E., Lee, J.-M., Killiany, R.J., Rosene, D.L., Kim, D.-S., Ronen, I., 2012. Age-related effects on cortical thickness patterns of the Rhesus monkey brain, 200.e23-200.e31 Neurobiol. Aging 33. https://doi.org/10.1016/j.neurobiolaging.2010.07.010.
Kubicki, M., Baxi, M., Pasternak, O., Tang, Y., Karmacharya, S., Chunga, N., Lyall, A.E., Rathi, Y., Eckbo, R., Bouix, S., Mortazavi, F., Papadimitriou, G., Shenton, M.E., Westin, C.F., Killiany, R., Makris, N., Rosene, D.L., 2019. Lifespan trajectories of white matter changes in rhesus monkeys. Cereb. Cortex 29, 1584–1593. https://doi.org/10.1093/cercor/bhy056.
Lebel, C., Beaulieu, C., 2011. Longitudinal development of human brain wiring continues from childhood into adulthood. J. Neurosci. 31, 10937–10947. https://doi.org/10.1523/JNEUROSCI.5302-10.2011.
Lebel, C., Walker, L., Leemans, A., Phillips, L., Beaulieu, C., 2008. Microstructural maturation of the human brain from childhood to adulthood. NeuroImage 40, 1044–1055. https://doi.org/10.1016/j.neuroimage.2007.12.053.
Levakov, G., Rosenthal, G., Shelef, I., Raviv, T.R., Avidan, G., 2020. From a deep learning model back to the brain—identifying regional predictors and their relation to aging. Hum. Brain Mapp. 41, 3235–3252. https://doi.org/10.1002/hbm.25011.
Madan, C.R., 2015. Creating 3D visualizations of MRI data: A brief guide. F1000Research 4, 466.
Madan, C.R., 2019. Shape-related characteristics of age-related differences in subcortical structures. Aging Ment. Health 23, 800–810. https://doi.org/10.1080/13607863.2017.1421613.
Madan, C.R., Kensinger, E.A., 2018. Predicting age from cortical structure across the lifespan. Eur. J. Neurosci. 47, 399–416. https://doi.org/10.1111/ejn.13835.
Madan, C.R., Kensinger, E.A., 2017. Age-related differences in the structural complexity of subcortical and ventricular structures. Neurobiol. Aging 50, 87–95. https://doi.org/10.1016/j.neurobiolaging.2016.10.023.
Madhavan, K.M., McQueeny, T., Howe, S.R., Shear, P., Szaflarski, J., 2014. Superior longitudinal fasciculus and language functioning in healthy aging. Brain Res 1562, 11–22. https://doi.org/10.1016/j.brainres.2014.03.012.
Makris, N., Kennedy, D.N., Boriel, D.L., Rosene, D.L., 2010. Methods of MRI-based structural imaging in the aging monkey. Methods, MRI Nonhum. Primate Brain 50, 166–177. https://doi.org/10.1016/j.ymeth.2009.06.007.
Makris, N., Papadimitriou, G.M., van der Kouwe, A., Kennedy, D.N., Hodge, S.M., Dale, A.M., Benner, T., Wald, L.L., Wu, O., Tuch, D.S., Caviness, V.S., Moore, T.L., Killiany, R.J., Moss, M.B., Rosene, D.L., 2007. Frontal connections and cognitive changes in normal aging rhesus monkeys: A DTI study. Neurobiol. Aging 28, 1556–1567. https://doi.org/10.1016/j.neurobiolaging.2006.07.005.
Mattison, J.A., Colman, R.J., Beasley, T.M., Allison, D.B., Kemnitz, J.W., Roth, G.S., Ingram, D.K., Weindruch, R., de Cabo, R., Anderson, R.M., 2017. Caloric restriction improves health and survival of rhesus monkeys. Nat. Commun. 8, 14063 https://doi.org/10.1038/ncomms14063.
Moore, T.L., Killiany, R.J., Herndon, J.G., Rosene, D.L., Moss, M.B., 2006. Executive system dysfunction occurs as early as middle-age in the rhesus monkey. Neurobiol. Aging 27, 1484–1493. https://doi.org/10.1016/j.neurobiolaging.2005.08.004.
Moss, M.B., Killiany, R.J., Herndon, J.G., 1999. Age-Related Cognitive Decline in the Rhesus Monkey. In: Peters, A., Morrison, J.H. (Eds.), Cerebral Cortex: Neurodegenerative and Age-Related Changes in Structure and Function of Cerebral Cortex, Cerebral Cortex. Springer US, Boston, MA, pp. 21–47. https://doi.org/10.1007/978-1-4615-4885-0_2.
Park, D.C., Lautenschlager, G., Hedden, T., Davidson, N.S., Smith, A.D., Smith, P.K., 2002. Models of visuospatial and verbal memory across the adult life span. Psychol. Aging 17, 299.
Passingham, R., 2009. How good is the macaque monkey model of the human brain? Curr. Opin. Neurobiol. 19, 6–11. https://doi.org/10.1016/j.conb.2009.01.002.
Petrides, M., Pandya, D. n, 2006. Efferent association pathways originating in the caudal prefrontal cortex in the macaque monkey. J. Comp. Neurol. 498, 227–251. https://doi.org/10.1002/cne.21048.
Raz, N., Ghisletta, P., Rodrigue, K.M., Kennedy, K.M., Lindenberger, U., 2010. Trajectories of brain aging in middle-aged and older adults: regional and individual differences. NeuroImage 51, 501–511. https://doi.org/10.1016/j.neuroimage.2010.03.020.
Raz, N., Lindenberger, U., Rodrigue, K.M., Kennedy, K.M., Head, D., Williamson, A., Dahle, C., Gerstorf, D., Acker, J.D., 2005. Regional brain changes in aging healthy adults: general trends, individual differences and modifiers. Cereb. Cortex 15, 1676–1689. https://doi.org/10.1093/cercor/bhi044.
Reagh, Z., Yassa, M., 2017. Selective vulnerabilities and biomarkers in neurocognitive aging. F1000Research 6.
Sala, S., Agosta, F., Pagani, E., Copetti, M., Comi, G., Filippi, M., 2012. Microstructural changes and atrophy in brain white matter tracts with aging. Neurobiol. Aging 33, 488–498.e2. https://doi.org/10.1016/j.neurobiolaging.2010.04.027.
Salat, D.H., Buckner, R.L., Snyder, A.Z., Greve, D.N., Desikan, R.S.R., Busa, E., Morris, J.C., Dale, A.M., Fischl, B., 2004. Thinning of the cerebral cortex in aging. Cereb. Cortex N. Y. N. 1991 14, 721–730. https://doi.org/10.1093/cercor/bhh032.
Salat, D.H., Kaye, J.A., Janowsky, J.S., 2001. Selective preservation and degeneration within the prefrontal cortex in aging and Alzheimer disease. Arch. Neurol. 58, 1403–1408. https://doi.org/10.1001/archneur.58.9.1403.
Salat, D.H., Kaye, J.A., Janowsky, J.S., 1999. Prefrontal gray and white matter volumes in healthy aging and alzheimer disease. Arch. Neurol. 56, 338–344. https://doi.org/10.1001/archneur.56.3.338.
Salthouse, T.A., 2011. Neuroanatomical substrates of age-related cognitive decline. Psychol. Bull. 137, 753.
Sandell, J.H., Peters, A., 2003. Disrupted myelin and axon loss in the anterior commissure of the aged rhesus monkey. J. Comp. Neurol. 466, 14–30. https://doi.org/10.1002/cne.10859.
Sawiak, S.J., Picq, J.-L., Dhenain, M., 2014. Voxel-based morphometry analyses of in vivo MRI in the aging mouse lemur primate. Front. Aging Neurosci. 6 https://doi.org/10.3389/fnagi.2014.00082.
Sawiak, S.J., Shiba, Y., Oikonomidis, L., Windle, C.P., Santangelo, A.M., Grydeland, H., Cockcroft, G., Bullmore, E.T., Roberts, A.C., 2018. Trajectories and milestones of cortical and subcortical development of the marmoset brain from infancy to adulthood. Cereb. Cortex 28, 4440–4453. https://doi.org/10.1093/cercor/bhy256.
Schmachmann, Pandya, 2006. "Fiber Pathways of the Brain". Oxford University Press.
Schnack, H.G., Van Haren, N.E., Nieuwenhuis, M., Hulshoff Pol, H.E., Cahn, W., Kahn, R.S., 2016. Accelerated brain aging in schizophrenia: a longitudinal pattern recognition study. Am. J. Psychiatry 173, 607–616.
Shamy, J.L., Habeck, C., Hof, P.R., Amaral, D.G., Fong, S.G., Buonocore, M.H., Stern, Y., Barnes, C.A., Rapp, P.R., 2011. Volumetric correlates of spatiotemporal working and recognition memory impairment in aged rhesus monkeys. Cereb. Cortex 21, 1559–1573. https://doi.org/10.1093/cercor/bhq210.
Shamy, J.L.T., Buonocore, M.H., Makaron, L.M., Amaral, D.G., Barnes, C.A., Rapp, P.R., 2006. Hippocampal volume is preserved and fails to predict recognition memory impairment in aged rhesus monkeys (Macaca mulatta). Neurobiol. Aging 27, 1405–1415. https://doi.org/10.1016/j.neurobiolaging.2005.07.019.
Sherwood, C.C., Gordon, A.D., Allen, J.S., Phillips, K.A., Erwin, J.M., Hof, P.R., Hopkins, W.D., 2011. Aging of the cerebral cortex differs between humans and chimpanzees. Proc. Natl. Acad. Sci. 108, 13029–13034. https://doi.org/10.1073/pnas.1016709108.
Shobin, E., Bowley, M.P., Estrada, L.I., Heyworth, N.C., Orczykowski, M.E., Eldridge, S.A., Calderazzo, S.M., Mortazavi, F., Moore, T.L., Rosene, D.L., 2017. Microglia activation and phagocytosis: relationship with aging and cognitive impairment in the rhesus monkey. Geroscience 39, 199–220.
Sivera, R., Delingette, H., Lorenzi, M., Pennec, X., Ayache, N., 2019. A model of brain morphological changes related to aging and Alzheimer's disease from cross-sectional assessments. NeuroImage 198, 255–270. https://doi.org/10.1016/j.neuroimage.2019.05.040.
Small, B.J., Dixon, R.A., McArdle, J.J., 2011. Tracking cognition–health changes from 55 to 95 years of age. J. Gerontol. B. Psychol. Sci. Soc. Sci. 66, i153–i161.
Sowell, E.R., Peterson, B.S., Kan, E., Woods, R.P., Yoshii, J., Bansal, R., Xu, D., Zhu, H., Thompson, P.M., Toga, A.W., 2007. Sex differences in cortical thickness mapped in 176 healthy individuals between 7 and 87 years of age. Cereb. Cortex 17, 1550–1560. https://doi.org/10.1093/cercor/bhl066.
Sridharan, A., Willette, A.A., Bendlin, B.B., Alexander, A.L., Coe, C.L., Voytko, M.L., Colman, R.J., Kemnitz, J.W., Weindruch, R.H., Johnson, S.C., 2012. Brain volumetric and microstructural correlates of executive and motor performance in aged rhesus monkeys. Front. Aging Neurosci. 4 https://doi.org/10.3389/fnagi.2012.00031.
Stonebarger, G., Urbanski, H., Woltjer, R., Vaughan, K., Ingram, D., Schultz, P., Calderazzo, S., Siedeman, J., Mattison, J., Rosene, D., Kohama, S., 2020. Amyloidosis increase is not attenuated by long-term calorie restriction or related to neuron density in the prefrontal cortex of extremely aged rhesus macaques. GeroScience 42, 1733–1749. https://doi.org/10.1007/s11357-020-00259-0.
Taki, Y., Goto, R., Evans, A., Zijdenbos, A., Neelin, P., Lerch, J., Sato, K., Ono, S., Kinomura, S., Nakagawa, M., Sugiura, M., Watanabe, J., Kawashima, R., Fukuda, H., 2004. Voxel-based morphometry of human brain with age and cerebrovascular risk factors. Neurobiol. Aging 25, 455–463. https://doi.org/10.1016/j.neurobiolaging.2003.09.002.
Tigges, J., Gordon, T.P., McClure, H.M., Hall, E.C., Peters, A., 1988. Survival rate and life span of rhesus monkeys at the Yerkes Regional Primate Research Center. Am. J. Primatol. 15 (3), 263–273.
Taki, Y., Thyreau, B., Kinomura, S., Sato, K., Goto, R., Kawashima, R., Fukuda, H., 2011. Correlations among brain gray matter volumes, age, gender, and hemisphere in healthy individuals. PLOS ONE 6, e22734. https://doi.org/10.1371/journal.pone.0022734.
Tisserand, D.J., Pruessner, J.C., Sanz Arigita, E.J., van Boxtel, M.P.J., Evans, A.C., Jolles, J., Uylings, H.B.M., 2002. Regional frontal cortical volumes decrease

differentially in aging: an MRI study to compare volumetric approaches and voxel-based morphometry. NeuroImage 17, 657–669.
Uematsu, A., Hata, J., Komaki, Y., Seki, F., Yamada, C., Okahara, N., Kurotaki, Y., Sasaki, E., Okano, H., 2017. Mapping orbitofrontal-limbic maturation in non-human primates: A longitudinal magnetic resonance imaging study. NeuroImage 163, 55–67. https://doi.org/10.1016/j.neuroimage.2017.09.028.
Uno, H., 1993. The incidence of senile plaques and multiple infarction in aged Macaque brain. Neurobiol. Aging 14, 673–674. https://doi.org/10.1016/0197-4580(93)90067-L.
Walhovd, K.B., Westlye, L.T., Amlien, I., Espeseth, T., Reinvang, I., Raz, N., Agartz, I., Salat, D.H., Greve, D.N., Fischl, B., 2011. Consistent neuroanatomical age-related volume differences across multiple samples. Neurobiol. Aging 32, 916–932.
Wenk, G.L., Pierce, D.J., Struble, R.G., Price, D.L., Cork, L.C., 1989. Age-related changes in multiple neurotransmitter systems in the monkey brain. Neurobiol. Aging 10, 11–19. https://doi.org/10.1016/S0197-4580(89)80005-3.
Westlye, L.T., Walhovd, K.B., Dale, A.M., Bjørnerud, A., Due-Tønnessen, P., Engvig, A., Grydeland, H., Tamnes, C.K., Ostby, Y., Fjell, A.M., 2010. Life-span changes of the human brain white matter: diffusion tensor imaging (DTI) and volumetry. Cereb. Cortex N. Y. N. 1991 20, 2055–2068. https://doi.org/10.1093/cercor/bhp280.
Wisco, J.J., Killiany, R.J., Guttmann, C.R., Warfield, S.K., Moss, M.B., Rosene, D.L., 2008. An MRI study of age-related white and gray matter volume changes in the rhesus monkey. Neurobiol. Aging 29, 1563–1575.